Lab on a Chip

Miniaturisation for chemistry, physics, biology, materials science and bioengineering

www.rsc.org/loc

Volume 12 | Number 21 | 7 November 2012 | Pages 4195–4582

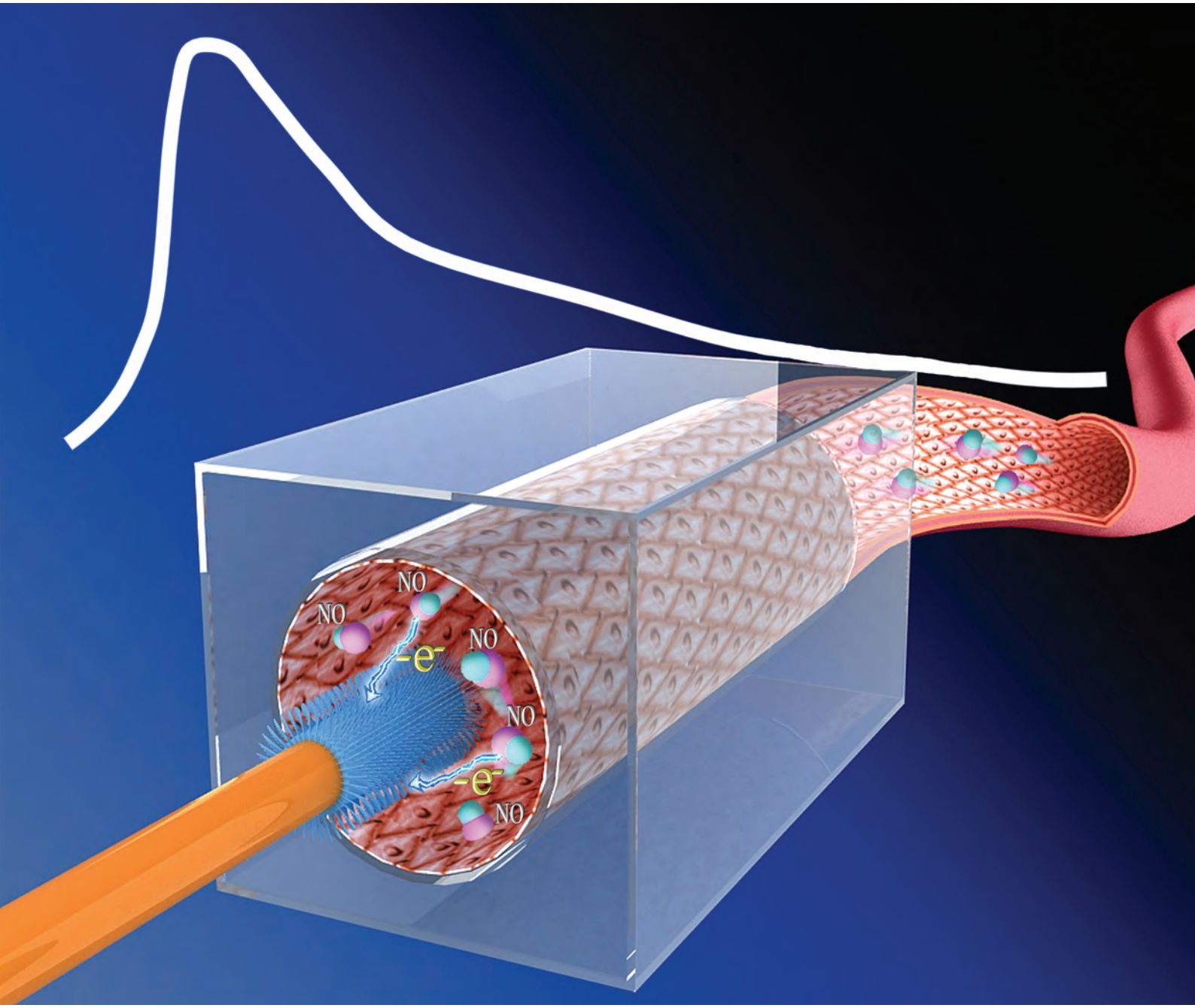

ISSN 1473-0197

RSC Publishing

PAPER

Wei-Hua Huang, Kai-Fu Huo *et al.*

Vascular lumen simulation and highly-sensitive nitric oxide detection using three-dimensional gelatin chip coupled to TiC/C nanowire arrays microelectrode

1473-0197(2012)12:21;1-Z

Lab on a Chip

Dynamic Article Links

Cite this: *Lab Chip*, 2012, **12**, 4249–4256

www.rsc.org/loc

PAPER

Vascular lumen simulation and highly-sensitive nitric oxide detection using three-dimensional gelatin chip coupled to TiC/C nanowire arrays microelectrode†

Lin-Mei Li,‡[a] Xue-Ying Wang,‡[a] Liang-Sheng Hu,[b] Rong-Sheng Chen,[b] Ying Huang,[a] Shi-Jing Chen,[a] Wei-Hua Huang,*[a] Kai-Fu Huo*[bc] and Paul K. Chu[c]

Received 10th February 2012, Accepted 5th July 2012
DOI: 10.1039/c2lc40148g

Reproducing the physiological environment of blood vessels for the *in vitro* investigation of endothelial cell functions is very challenging. Here, we describe a vascular-like structure based on a three-dimensional (3D) gelatin chip with good compatibility and permeability which is also cost-effective and easy to produce. The controllable lumen diameter and wall thickness enable close mimicking of blood vessels *in vitro*. The 3D gelatin matrix between adjacent lumens is capable of generating soluble-factor gradients inside, and diffusion of molecules with different molecular weights through the matrix is studied. The cultured human umbilical vein endothelial cells proliferate on the gelatin lumen linings to form a vascular lumen. The hemodynamic behavior including adhesion, alignment of endothelial cells (ECs) under shear stress and pulsatile stretch is studied. Furthermore, a microelectrode comprising TiC/C nanowire arrays is fabricated to detect nitric oxide with sub-nM detection limits and NO generation from the cultured ECs is monitored in real time. This vascular model reproduces the surrounding parenchyma of endothelial cells and mimics the hemodynamics inside blood vessels very well, thereby enabling potential direct investigation of hemodynamics, angiogenesis, and tumor metastasis *in vitro*.

Introduction

Blood vessels such as arteries, veins, and capillaries consisting of endothelial cells, smooth muscle cells and fibroblasts constitute the most important parts of the circulatory system. Endothelial cells (ECs) are composed of a biologically active cellular monolayer lining the blood vessel surface and deliver a variety of physiological and pathological vascular responses.[1] Investigation of the structure and functions of blood vessels and ECs based on many considerations such as hemodynamics is of great scientific importance.[2–5] Various fabrication techniques and materials have been used to produce ideal *in vitro* EC culturing systems and vascular simulation models. Flexible silicone tubes were initially used to simulate blood vessel lumens,[6,7] but the materials usually have poor compatibility and permeability. Recently, based on soft lithography[8,9] and replica molding of elastomeric materials such as poly(dimethylsiloxane) (PDMS), microfluidic devices have been developed as powerful and versatile tools to mimic blood vessels.[10] In this microfluidics technique, various *in vitro* EC culturing systems were successfully developed and different fluid flow, pressure, and stretch can be easily generated. In order to investigate the diagnosis and treatment of vascular disease, EC models were used to study a variety of effects generated by mechanical stress such as pressure, strain, and shear stress associated with normal and pathological flow states.[11–13] ECs are usually cultured on PDMS membranes enabling reconstitution of functional interfaces of the human organs,[14–16] which would accelerate pharmaceutical development. Simultaneously, the cell adhesion and permeability assays, transport and pathophysiological properties could also be investigated.[17–19]

However, PDMS suffers from strong hydrophobicity and poor compatibility.[20] Although various ways exist to facilitate cell attachment on PDMS surface, such as surface grafting and coating with proper extracellular matrixes (ECMs), the extensive application of PDMS to imitate 3D cell growth is still limited owing to its non-bioactivity.[21,22] Furthermore, as a dense aperture polymer, permeability to a variety of soluble factors is not desirable. The influence of kinds of factors on ECs cannot be reproduced and important cellular behavior such as angiogenesis can hardly be investigated. In this respect, hydrogels with better

[a]*Key Laboratory of Analytical Chemistry for Biology and Medicine (Ministry of Education), College of Chemistry and Molecular Sciences, Wuhan University, Wuhan, 430072, China. E-mail: whhuang@whu.edu.cn; Fax: +86 27 68754067*
[b]*College of Chemical Engineering and Technology and School of Materials and Metallurgy, Wuhan University of Science and Technology, Wuhan, 430081, China. E-mail: kfhuo@wust.edu.cn*
[c]*Department of Physics and Materials Science, City University of Hong Kong, Tat Chee Avenue, Kowloon, Hong Kong, China*
† Electronic Supplementary Information (ESI) available: Fig. S1, S2 and S3, Supplementary movies AVI and WMV. See DOI: 10.1039/c2lc40148g
‡ These two authors contributed equally to this paper.

biocompatibility and permeability provide a three-dimensional (3D) microenvironment for cell culture[23–26] and the embedded microstructures for EC culture can also be remolded by soft lithography.[27–29] However, a well-sealed hydrogel lumen is difficult to make due to the inability to bond the two cross-linked hydrogel chips. The physical microenviroment required by ECs *in vitro* and the various fluid flow, pressure, and stretch germane to blood vessels cannot be easily reproduced and this has hampered the use of hydrogel microfluidic devices in vascular simulation. Recently, some special technologies such as electrospinning and self-assembled monolayers were used in hydrogel based blood vessel simulation.[30–32] However, these methods required special and complex manipulations. Therefore, it is both important and challenging to develop a versatile, cost-effective, and easy-to-produce vascular model capable of both mimicking the 3D cellular microenvironment while being able to withstand the strong fluid stress in vascular simulation studies.[33]

Nitric oxide (NO) released from various cell types such as endothelial cells plays a crucial role in the biological functions of blood vessels such as vascular smooth muscle relaxation, platelet aggregation, and immune response.[34] The free radical molecular NO has a short lifetime and so the ability to accurately monitor minute NO concentrations in real time is vital to a better understanding of the pathophysiology related to blood vessels.[35] Electrochemical detection may provide real-time monitoring of NO generation in the physiological environment.[36] In order to improve sensitivity and selectivity for NO detection, several different types of electrochemical sensors have been developed based on common materials including carbon,[37,38] platinum[39] and gold.[40] Shibuki fabricated a NO-selective microelectrode for detecting NO release in brain tissue, showing no sensitivity to oxygen or to oxidized derivatives of NO.[41] Afterwards, catalysts or nanomaterials[42–44] were used for modifying the electrode to increase its sensitivity, and gas-permeable membranes were used for improving selectivity.[45] Schoenfisch's group reported a fluorinated xerogel-derived microelectrode with a detection limit of 83 pM for NO detection.[46] Recently, microelectrode integrated microfluidic chips have been developed for NO detection from ECs secretions *in vitro*.[47–49] However, incorporation of both high sensitivity and good selectivity electrochemical sensors into microfluidic chips is still challenging.

In this paper, we describe a versatile, cost-effective, and easy-to-make microfluidic EC culture and NO monitoring model for vascular simulation. As the hydrolyzate of collagen, gelatin is rich in variety of nutrients required for cell growth and possesses excellent biocompatibility and bioactivity. The use of gelatin hydrogels enables easy remolding of lumen or lumen arrays with controllable diameter and wall thickness to reproduce the surrounding parenchyma of endothelial cells and generate a soluble factor gradient in the 3D matrix. A vascular-like lumen structure is produced by the EC culture, and different fluid flow, stress, and stretch can be generated to investigate the hemodynamics. Last but not least, highly sensitive and real-time monitoring of NO generation from the vascular-like lumen is demonstrated using a microelectrode composed of core–shell TiC/C nanowire arrays.

Materials and methods

Materials and reagents

The cell culture medium RPMI 1640 for EC culture was purchased from GIBCO (USA) and L-glutamine and HEPES were purchased from Amresco (USA). 3′,6′-Di(*O*-acetyl)-4′,5′-bis[*N*,*N*-bis(carboxymethyl)-aminomethyl] fluorescein, tetraacetoxymethylester(Calcein-AM), and 3,8-diamino-5-[3-(diethylmethylammonio)propyl]-6-phenylphenanthridinium diiodide (PI) for cell staining were obtained from Dojindo laboratory (USA). 4-Amino-5-methylamino-2′,7′-difluorofluorescein diacetate (DAM-FM DA) for NO fluorescent imaging was purchased from Beyotime (China). The gelatin, adenosine triphosphate (ATP), and nafion were purchased from Sigma (USA). All other chemicals unless specified were reagent grade and used without further purification.

Fabrication of gelatin lumen chip

The novel vascular simulation model consists of a peristaltic pump to manipulate flow and a cell culture gelatin chip with lumen or lumen arrays. The process to prepare the gelatin chips is shown in Scheme 1 and described as follows:

1. A plastic frame mold with a number of holes (the diameter and distance between adjacent holes could be controlled down to 100 μm) was fabricated (Scheme 1A).

2. Certain numbers of quartz capillaries with different sizes (100 μm to 1 mm) and shape (square or circular, depending on the requirements of the experiments) were inserted into the plastic frame mold and immobilized (Scheme 1B).

3. A 12.5% gelatin solution dissolved in phosphate buffer saline (PBS) was heated and the temperature was kept lower than 70 °C. 2 μL of trichloromethane were added to the gelatin solution for sterility and the gelatin solution was mixed evenly with a 10% transglutaminase solution. The mixed solution was poured into the plastic mold immobilized with the quartz capillaries and maintained in a humidified incubator at 37 °C for 2 h for gelatin cross-linking (Scheme 1C).

4. The capillaries were pulled out and the gelatin chip (Scheme 1D) was placed on a Petri dish. Polyethylene tubes with needles were used at both the inlet and outlet for interfacing and they were sealed with gelatin.

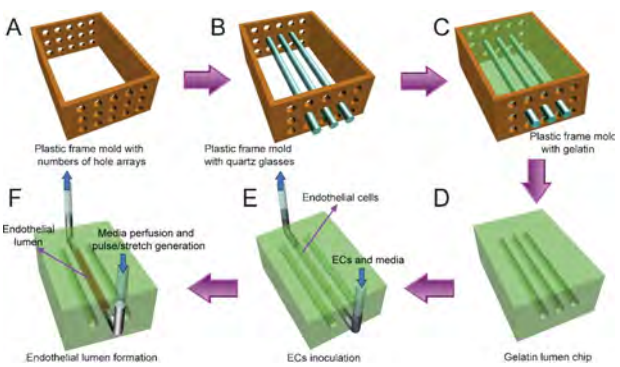

Scheme 1 Schematic diagram showing the fabrication of gelatin chip for vascular lumen simulation.

5. The ECs were seeded and cultured on the lining of the gelatin chip for the forming of vascular-like structure (Scheme 1E,F).

6. All the polyethylene tubes, needles, and molds were soaked in 75% (*v*/*v*) ethanol for 2 h and then exposed to ultra-violet (UV) light overnight in a clean hood before use.

Fabrication of core–shell titanium carbide/carbon nanowire (TiC/C NW) arrays microelectrode

Core–shell titanium carbide/carbon nanowire (TiC/C NW) arrays were fabricated by a thermochemical process as described previously.[50] In summary, titanium alloy (Ti6Al4V) wires (100 μm, Goodfellow) were degreased ultrasonically in acetone and ethanol sequentially, followed by etching to ~20 μm in a solution containing H_2O, HF and HNO_3 with a volume ratio of 5 : 1 : 4 for 8–10 min. After rinsing with double-distilled water and drying under flowing nitrogen, the Ti6Al4V wires were loaded onto a ceramic substrate placed at the center of an alumina tube in a horizontal tube furnace. The reactor was purged with pure argon several times to remove residual oxygen and moisture before being heated to 800 °C under Ar. Acetone was then introduced into the chamber together with argon at a flow rate of 150 sccm. The thermal chemical reaction was conducted for 90 min at 800 °C and then the furnace was gradually cooled to room temperature under Ar.

The fabricated TiC/C NW arrays (1 cm in length and 20 μm in diameter) were connected to a copper wire and insulated by curing silastic. The microelectrode consisting of the TiC/C NW arrays with an active length about 2–3 mm was obtained. A saturated NO solution ($c \approx 1.8$ mM)[34] was prepared according to a previously reported protocol.[51] The standard NO solution was prepared by gradual dilution of the saturated solution with deoxygenated PBS (pH = 7.2). To eliminate the anion interferences during detection, the microelectrode was immersed in 1% nafion for 5 s, dried for 5 min under air, and the process was repeated 9 times before NO detection. The morphology and structure of the microelectrode were determined by field-emission scanning electron microscopy (FE-SEM, FEI Nova 400 Nano) and transmission electron microscopy (TEM, JEOL JEM-2100, Japan). The composition of the microelectrode was determined by X-ray diffraction using the Cu-Kα radiation (λ = 1.5418 Å) (XRD, Philips X'Pert Pro, Netherland) and Raman scattering (Renishaw 2000, UK).

The microelectrode composed of TiC/C NW arrays was electrochemically characterized using $K_3[Fe(CN)_6]$ and NO on a CHI 660A electrochemical workstation (CH instruments Inc.) in a three-electrode arrangement including a TiC/C NW array working electrode, a Pt counter electrode and an Ag/AgCl reference electrode. All the electrochemical experiments were performed in a Faraday cage at room temperature (25 °C).

Human endothelial cell culture in gelatin lumen

The human umbilical vein endothelial cell line ECV 304 (China center for type culture collection, CCTCC, Wuhan, China) was used. The cells were routinely cultured using RPMI 1640 culture medium with 12% fetal bovine serum, 0.292 mg mL^{-1} L-glutamine, 4.766 mg mL^{-1} HEPES, and 0.85 mg mL^{-1} $NaHCO_3$ in the culture flask. The cells were cultured for 4 days and then suspended in fresh medium with a density of 1×10^7 cells mL^{-1}. The elastic tubing and metal pipe were sterilized prior to use and interfaced the lumen *via* a syringe or peristaltic pump for fluid transport. The sterile gelatin lumen was washed with fresh RPMI 1640 medium and the ECs were slowly perfused into the lumen (Scheme 1E,F). After adherence, the ECs were cultured on the gelatin lining under static conditions (control) or laminar flow under pulsatile stretch. The medium was replaced twice a day under static culturing conditions in a CO_2 incubator (Heracell 150i, Thermo Scientific, USA). The ECs were cultured for 4–5 days to form the confluence state and cover the entire circular lumen. The hemodynamical experiment results including the adherence ability, shear stress adaptation, and pulsatile strain manipulation of the ECs were obtained by an automated live cell imaging system (AxioObserver Z1 fluorescent microscope with camera and incubation system, ZEISS, Germany). The microscopic pictures of ECs cultured in a circular gelatin lumen under static conditions were observed using a Revolution XD confocal microscope (Andor) at 25 °C. The laminar or pulsatile fluids were generated by a syringe or peristaltic pump (Lange, China). The viability of the cultured cells was checked by injection of Calcein-AM and PI from the inlet to label the cells.

Shear stress evaluation and pulsatile flow generation

The physical properties of the culture medium were applied to the fluids used in the simulation and pulsation was generated by a peristaltic pump TS-2A (constant pump Co., Ltd. Baoding Lange). The Reynolds number at a flow rate of 20 mL min^{-1} in the quadrate channel with a cross-sectional area of 800 μm × 800 μm was estimated to be about 40, indicating a viscous laminar flow in which the fluid streamlines are steady and predictable. The cross-sectional aspect ratio, $\alpha = h/w$ = 800 μm / 800 μm = 1 and for systems that employ parallel flat plates separated by a narrow gap of height h, the wall shear stress τ_w can be calculated by:

$$\tau_w = 6\mu Q/wh^2$$

where Q is the flow rate, μ is the fluid viscosity, h and w are the height and width of the channels respectively.

Amperometric detection and fluorescence imaging of ATP-stimulated NO releasing from ECs cultured in gelatin lumen

The amperometric measurements were conducted in a temperature-controlled chamber (25 °C for the NO detection) using an inverted microscope (Axiovert 200M, Zeiss, Göttingen, Germany) placed in a Faraday cage. When the ECs were cultured to the confluent state and covered the entire inner surface in a circular gelatin lumen, the nutrient solution in the gelatin lumen was replaced by PBS and the gelatin chip was fixed on a Petri dish. One end of the gelatin lumen was used as the inlet of the stimulating solution and the outlet was used for electrochemical detection. The TiC/C NW arrays microelectrode was inserted inside the lumen outlet about 0.5 mm by a micromanipulator (TransferMan NK2, Eppendorf, Hamburg, Germany) and NO generation from the ECs was amperometrically monitored on a CHI 660A workstation at a constant potential of +0.75 V.

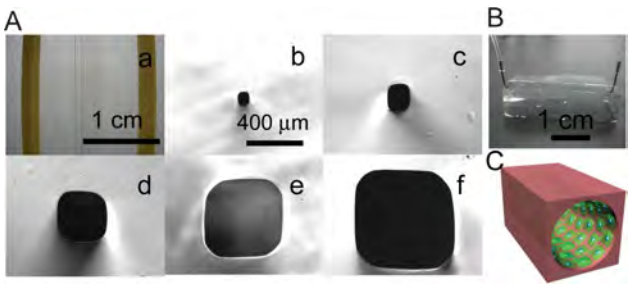

Fig. 1 (A) Photographs of the gelatin chip with five microlumens. The width of microchannels b to f is 100 μm, 200 μm, 400 μm, 600 μm, and 800 μm respectively; (B) Photograph of the interfaced gelatin chip for cell culture; (C) Schematic picture showing the simulated vascular lumen for EC culture.

When the ECs were cultured for 2 days, 100 μM DAF-FM DA solution was perfused into the lumen for 30 min incubation with the ECs, and then PBS was introduced into the lumen to remove the DAF-FM DA solution. Afterwards, the stimulant was perfused into the lumen to induce NO generation, and the fluorescence imaging was performed under an AxioObserver Z1 fluorescent microscope.

Results and discussion

Microfluidic device remolding and gradient generation for vascular lumen simulation

The EC adherence and proliferation behavior on several common hydrogels such as agarose, gelatin, matrigel, and sodium alginate were studied, and the replication ability of these hydrogels was also compared. Possessing excellent cell adherence/proliferation (Fig. S1†) and structure replication ability, gelatin was finally chosen as the material to remodel blood vessels. By using a plastic frame and quartz capillaries as the template (Scheme 1), a gelatin chip with integrated microlumen arrays inside was reproduced (Fig. 1B and C). The lumen size which depends on the diameter of the quartz capillary can be controlled (Fig. 1A b–f shows five square lumens with widths from 100 to 800 μm). Furthermore, the gelatin thickness between adjacent lumens can be regulated down to 100 μm and therefore arteries, veins and even capillaries can be mimicked *in vitro* using this model.

To simulate the permeability of the vessel and diffusion of soluble factors in the extravascular space, the gradient generation of molecules with different molecular weights (FITC-labeled dextran, Mw = 500 kDa and rhodamine-labeled dextran, M_w = 70 kDa) between gelatin lumens was investigated (Fig. 2A). The results showed that the gradient stabilizes to form an equilibrium profile and the profile depends on the molecular weight of the soluble factors. Molecules with a smaller molecular weight diffuse more easily across the 3D gelatin framework (Fig. 2B,C).

Proliferation of ECs and hemodynamical studies

The ECs adhered quickly (within 30 min) onto the inner surface (without surface pretreatment) of the gelatin lumen and started to proliferate after inoculation. After culturing for 4–5 days under static conditions, the ECs proliferated and covered almost all the gelatin lining, and grew along the wall to form an EC covered vascular lumen (Fig. 3A and Supplementary movie AVI†). We can increase the cell density and seed the cells twice to accelerate EC vascular formation. After seeding the ECs at the lumen bottom to let them adhere for 1 h, the chip was turned

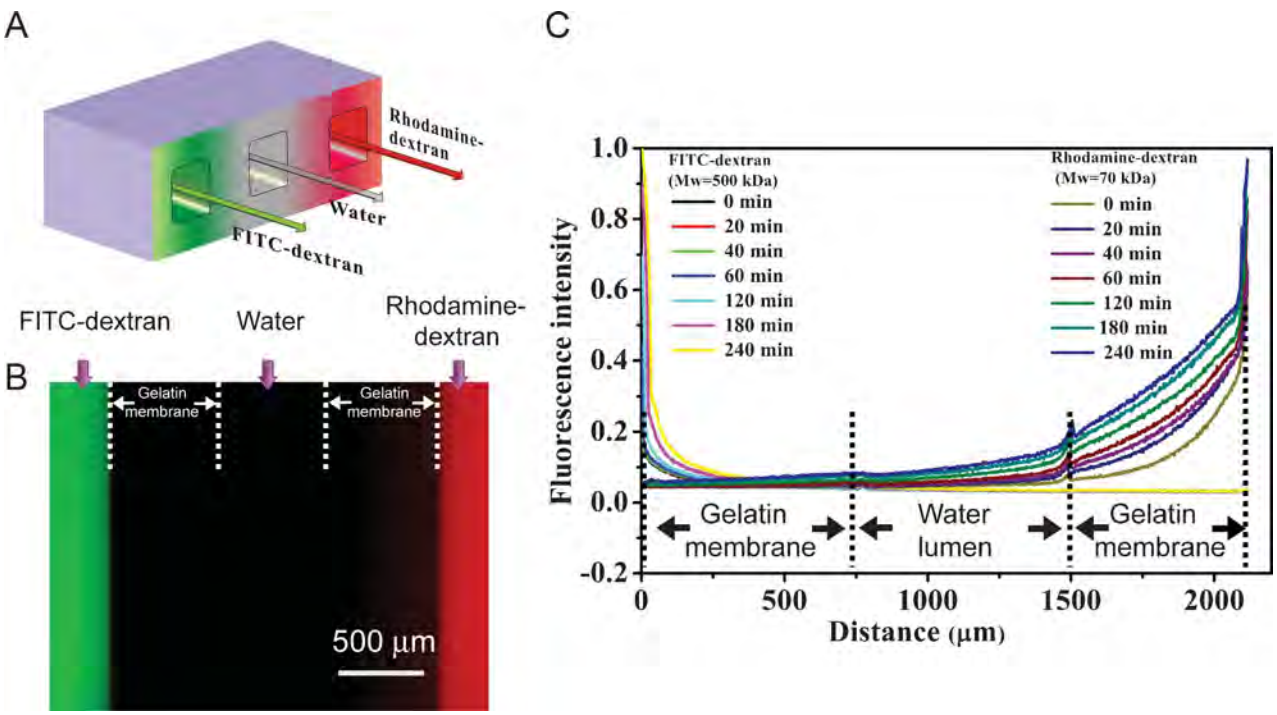

Fig. 2 (A) Schematic diagram showing the gradient generation of FITC-dextran (Mw = 500 kDa) and Rhodamine-dextran (M_w = 70 kDa) between adjacent gelatin lumens; (B) Fluorescence microscopy picture of gradient diffusion; (C) Development of concentration gradient profiles over time.

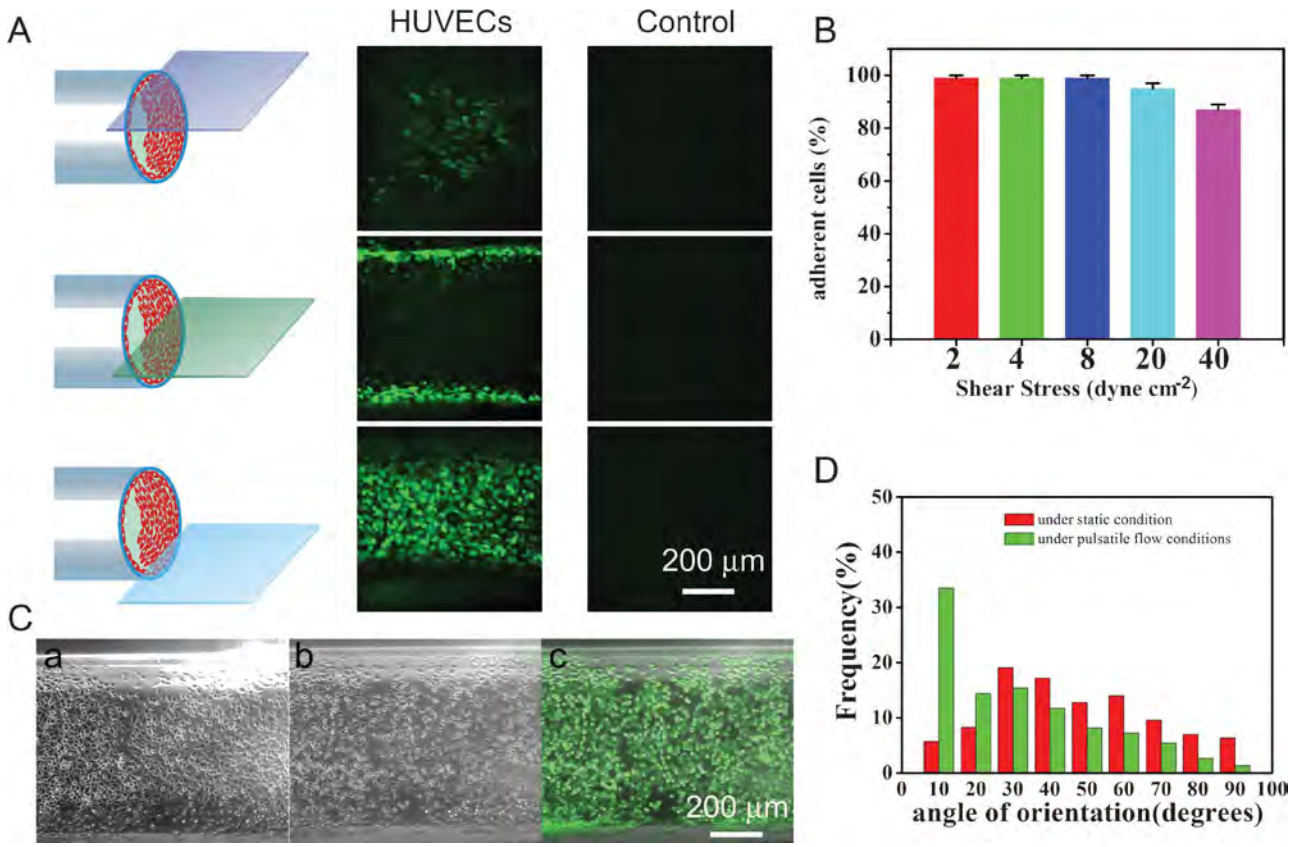

Fig. 3 (A) Microscopic pictures of ECs cultured in a circular gelatin lumen after 5 days under static conditions retracted from Z-stack model using a Revolution XD confocal microscope. The three rows represent the ECs (left panel) and a positive control (right panel) at the three typical layer positions; (B) Adherence of ECs under different shear stress after 0.5 h; (C) Microscopic pictures of ECs under pulsatile flow conditions (frequency 1 Hz and flow rate 5.5 mL), a: ECs cultured under static condition for 1 day after inoculation using a higher density, b: ECs cultured under pulsatile flow condition after 24 h and (c) labeled with Calcein-AM and PI; (D) Frequency of the angle of orientation of the ECs under pulsatile flow conditions after 20 h (frequency 1 Hz, flow rate 1.3 mL). The orientation angle (θ) is defined as the angle between the major axis of the best-fit ellipse around a cell and the direction of flow.

upside down for a second seeding, and the EC covered lumen could be formed in 1–2 days. Viability experiments using Calcein-AM and PI to label the ECs showed there were nearly no dead cells, further indicating excellent cytocompatibility of gelatin in rebuilding the 3D environment required by the ECs *in vivo*.

The adhesion ability of ECs onto the lumen lining and their hemodynamical characteristics such as adherence strength and adaptive response to shear stress were further investigated. The ECs exhibit strong adherent ability on the gelatin surface under different shear stress. The ECs appeared to be in the retraction state under a shear stress of 20 dyne cm^{-2}, and only 13% of the cells detached from the lumen surface under a shear stress of 40 dyne cm^{-2} after 0.5 h. This is more than the normal shear stress in veins and arteries (Fig. 3B). The results demonstrate the validity of the EC culture and vascular simulation model under strong shear stress tolerance and adaptation, and this is important to the structure and maintaining the functions of the ECs *in vitro*.

Cyclic strain-induced alignment of ECs under pulsatile flow was studied. Since the gelatin chip and gelatin membrane between adjacent lumens are elastic, the pulsatile pressure leads to cyclic strain of the gelatin lumen and adherent ECs on the lining. At a pulsing frequency of 1 Hz and a flow rate from 1.3 to 5.5 mL min^{-1}, the shear stress was in the range of 3–13 dyne cm^{-2}, representing the average shear stress in veins and arteries. Under the dual effects of shear stress and cyclic strain, the ECs began to align parallel to the direction of the flow and elongate to different aspect ratios (Fig. 3C). Quantitative analysis showed a uniform distribution of the orientation angle after culturing under static conditions for 1 day, whereas the orientation angle of 63% of the cells was skewed less than 30° after 20 h under a pulsatile flow at a frequency of 1 Hz and flow rate of 1.3 mL min^{-1} (Fig. 3D, Supplementary movie WMV†). The alignment result is not comparable to that reported on a PDMS membrane[15] due to the strong adherence of ECs on the gelatin surface invading parts of the matrix.[28]

Characterization of TiC/C NW arrays microelectrode

Core–shell TiC/C NW arrays produced directly on a Ti6Al4V foil by a thermochemical process show excellent electrochemical and biocompatibility behavior.[52] Here, we use Ti6Al4V wires (100 μm in diameter) as the starting materials and fabricate a microelectrode composed of core–shell TiC/C nanowire (TiC/C NW) arrays that can be inserted into the gelatin lumen as a detector. SEM shows a 25 μm diameter microelectrochemical

sensor with nanowire arrays coated on the surface (Fig. 4A,B). The TEM image (Fig. 4B) reveals that the nanowire has a core–shell (TiC/C) structure and XRD indicates that the main diffraction peaks, except the peaks from the substrate, can be indexed to cubic TiC[53,54] (Fig. 4C). The two strong Raman peaks at 1343 and 1592 cm^{-1} correspond to the D and G bands of carbon, respectively. Shifting of the G band from its normal value of 1580 to 1592 cm^{-1} indicates that the carbon shells are made of nanocrystalline graphite or sp^2 clusters (Fig. 4D). The large sp^2 content gives rise to excellent electron transfer and electron conductivity[55] and consequently larger specific surface area, and the high sp^2 content in the carbon shells yields highly sensitive electrochemical detection.

This sensor showed excellent electrochemical behavior (Fig. S2†) and NO detection capability, and the oxidation potential is +0.75 V *versus* the Ag/AgCl reference electrode (Fig. 5A). After modification with 1% nafion to eliminate interfering anions like nitrite (NO_2^-), uric acid (UA) and ascorbic acid (AA), the calculated selectivities for NO against nitrite, UA and AA were 625 : 1, 800 : 1 and 155 : 1 respectively, showing that this sensor had good selectivity over these potential interfering anions during biological measurements. The typical response time of this sensor to NO was about 400 ms (Fig. 5B), if we define the response time as the interval between the instant at which current reaches 10% of the maximum and the instant at which current rises to 90% of the maximum. The fast response characteristic of the sensor facilitates the real-time monitoring of NO events in cells. Furthermore, over the NO concentration range of interest (5–1000 nM), this sensor displays an excellent linear amperometric response (R^2 = 0.995) (Fig. 5C), and a detection limit (DL) of 0.6 nM (S/N = 3) (Fig. 5B) was achieved.

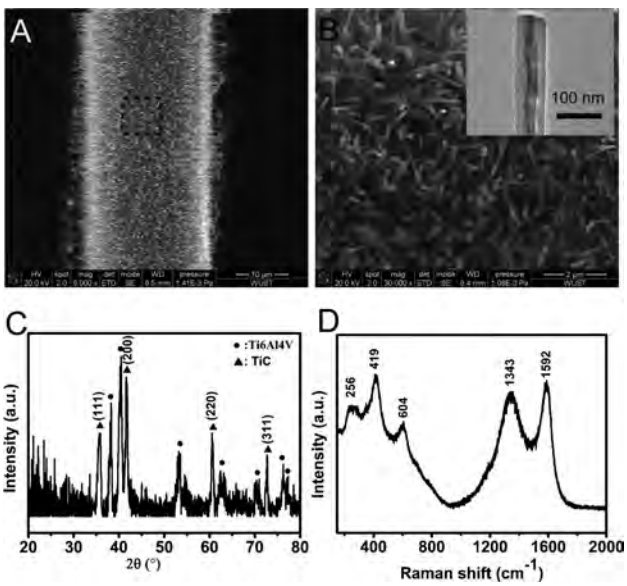

Fig. 4 (A,B) SEM images of TiC/C NW arrays microelectrode, (inset) enlarged image and TEM of a single TiC/C nanowire; (C) X-ray diffraction (XRD) pattern and (D) Raman results acquired from the TiC/C NW arrays microelectrode.

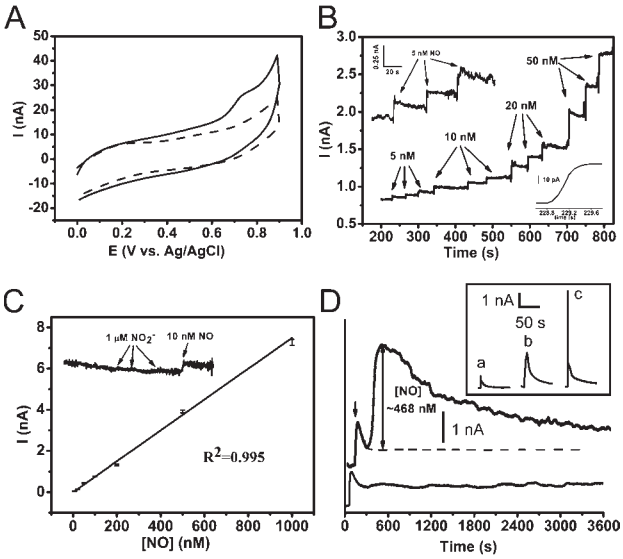

Fig. 5 (A) Cyclic voltammograms obtained from the TiC/C NW arrays microelectrode in PBS in the absence of NO (dashed line) and in the presence of 1.8 μM NO (solid line) at a scanning rate of 100 mV s^{-1}. (B) Amperometric responses to increases of NO concentrations in a stirred deaerated phosphate buffer saline (PBS). The amperometric response to 5 nM NO is magnified in the upper inset, and an amplified amperometric curve illustrating the sensor's response time to NO is in the lower inset. (C) Calibration curve for the NO solution over the concentration range of interest. Selectivity detection of NO_2^- and NO is shown in the inset. (D) Real-time amperometric detection without ECs (bottom panel) and with confluence ECs (upper panel) by introducing 100 μM ATP-stimulating from one end of the gelatin lumen at 5 μL min^{-1}. The arrows indicate baseline changes when ATP is introduced into the gelatin lumen. The top inset picture shows elevated NO level with increasing shear forces from 0.08 dyne cm^{-2}(a), to 0.33 dyne cm^{-2}(b), to 0.65 dyne cm^{-2}(c); the three measurements were performed inside another gelatin lumen and ECs were preincubated with 5 mM L-arginine for 30 min before each detection to maintain successive NO generation.

NO release from the simulated vascular lumen

When a confluent layer of ECs was formed and covered the entire gelatin lumen lining, one end of the lumen was used as the inlet in stimulating solution perfusion and the outlet was used for electrochemical detection. For a circular gelatin lumen with a diameter of 600 μm and length of 10 mm, it is estimated that the longest travel time for released NO from ECs to the electrode under a flow rate of 5 μl min^{-1} is about 28 s. This is less than the reported lifetime of NO (~200 s).[56] Stimulation using 100 μM ATP perfusion causes NO generation from the ECs inside the lumen. Amperometric detection showed a fast current increase within 120 s after ATP addition and then a slow decline to the baseline (upper trace in Fig. 5D, the small current peak before the NO signal was caused by the arrival of the perfusion flow at the electrode). The highest concentration of NO we detected was about 468 nM, which is higher than that previously reported. This is possibly because the 3D culture model uses this vascular simulation model where ECs cover the whole inner surface of the circular lumen, instead of previous models where ECs were cultured on only one plain surface.

Fluid shear stress is thought to cause the generation of NO.[57–59] Based on the vascular lumen model, NO generation under

different shear stresses was real-time detected. Three measurements were performed inside a gelatin lumen and ECs were preincubated with 5 mM L-arginine for 30 min before each detection to maintain successive NO generation. The results (inset in Fig. 5D) show elevated NO level with increasing shear forces from 0.08 dyne cm^{-2} (flow rate: 5 μL min^{-1}), 0.33 dyne cm^{-2} (flow rate: 20 μL min^{-1}) to 0.65 dyne cm^{-2} (flow rate: 40 μL min^{-1}). The maximum NO concentrations under the three shear forces are 256 nM, 861 nM and 1780 nM respectively. Larger shear force was not used, because the sensor was directly inserted into the outlet of the gelatin lumen, and electrode perturbation caused by high flow rate increased the background noise of the amperometric signal. Successful detection of NO levels change with alternative shear stresses demonstrated that this vascular model could possibly provide a useful technique to investigate NO-mediated vascular function *in vitro*.

NO generation from the cultured ECs inside gelatin lumen was further proved by fluorescent imaging using a cell-trappable fluorescent probe DAF-FM DA.[60] The results (Fig. S3†) showed that the fluorescent intensity was increased obviously during the perfusion stimulation, which is in good agreement with the amperometric results.

Conclusions

We fabricated a 3D gelatin lumen using a cost-effective and easy process for vascular simulation. Gelatin has the advantage of excellent cell adherence/proliferation and structure replication ability. The soluble factor gradient generation, EC adherence, proliferation, vascular lumen formation, and various hemodynamical properties were demonstrated. The NO production from the simulated blood vessel was monitored in real time by a sensitive microelectrode consisting of TiC/C NW arrays. This model can replicate the vascular microenviroment and hemodynamics inside the blood vessel and, in combination with the highly sensitive detection technique, provided the capability for *in vitro* investigation into such areas as hemodynamics, atherosclerosis, tumor metastasis, angiogenesis, and drug screening. One of the important outcomes of this study is real-time monitoring of cells in a mimicked cellular microenvironment *in vivo*.[61] This enables possible advances in mimicking the vascular environment using a poriferous hydrogel by introducing smooth muscle cells and ECs co-culture systems, and *in vitro* study of tumor metastasis and angiogenesis.

Acknowledgements

This work was supported by the National Natural Science Foundation of China (Nos. 20975077, 31070995, 50902104 and 21105077), the Science Fund for Creative Research Groups (No. 20921062), the National Basic Research Program of China (973 Program, No. 2007CB714507), the Program for New Century Excellent Talents in University (NCET-10-0611), the Program for Changjiang Scholars and Innovative Research Team in University (IRT1030), Hong Kong Research Grants Council (RGC) General Research Funds (GRF) No. CityU 112510, and City University of Hong Kong Strategic Research Grant (SRG) No. 7008009. The first two authors contributed equally to this work.

References

1 N. Resnick, H. Yahav, A. Shay-Salit, M. Shushy, S. Schubert, L. C. M. Zilberman and E. Wofovitz, *Prog. Biophys. Mol. Biol.*, 2003, **81**, 177–199.
2 S. Chien, *Am. J. Physiol.: Heart Circ. Physiol.*, 2007, **292**, H1209–H1224.
3 V. Vickerman, J. Blundo, S. Chung and R. Kamm, *Lab Chip*, 2008, **8**, 1468–1477.
4 J. A. Frangos, S. G. Eskin, L. V. McIntire and C. L. Ives, *Science*, 1985, **227**, 1477–1479.
5 C. L. Walsh, B. M. Babin, R. W. Kasinskas, J. A. Foster, M. J. McGarry and N. S. Forbes, *Lab Chip*, 2009, **9**, 545–554.
6 S. Zhao, A. Suciu, T. Ziegler, J. E. Jr. Moore, E. Burki, J. J. Meister and H. R. Brunner, *Arterioscler., Thromb., Vasc. Biol.*, 1995, **15**, 1781–1786.
7 X. Q. Peng, F. A. Recchia, B. J. Byrne, I. S. Wittstein, R. C. Ziegelstein and D. A. Kass, *Am. J. Physiol. Cell Physiol.*, 2000, **279**, C797–C805.
8 Y. Xia and G. M. Whitesides, *Angew. Chem., Int. Ed.*, 1998, **37**, 550–575.
9 T. Thorsen, S. J. Maerkl and S. R. Quake, *Science*, 2002, **298**, 580–584.
10 E. W. K. Young and C. A. Simmons, *Lab Chip*, 2010, **10**, 143–160.
11 G. A. Giridharan, M. D. Nguyen, R. Estrada, V. Parichehreh, T. Hamid, M. A. Ismahil, S. D. Prabhu and P. Sethu, *Anal. Chem.*, 2010, **82**, 7581–7587.
12 R. Estrada, G. A. Giridharan, M. D. Nguyen, T. J. Roussel, M. Shakeri, V. Parichehreh, S. D. Prabhu and P. Sethu, *Anal. Chem.*, 2011, **83**, 3170–3177.
13 L. Wang, Z. L. Zhang, J. W. Bakala, D. W. Pang, J. M. Liu and Y. Chen, *Lab Chip*, 2011, **11**, 4235–4240.
14 D. Huh, H. Fujioka, Y. C. Tung, N. Futai, R. Paine, J. B. Grotberg and S. Takayama, *Proc. Natl. Acad. Sci. U. S. A.*, 2007, **104**, 18886–18891.
15 D. Huh, B. D. Matthews, A. Mammoto, M. Montoya-Zavala, H. Y. Hsin and D. E. Ingber, *Science*, 2010, **328**, 1662–1668.
16 H. J. Kim, D. Huh, G. Hamiltona and D. E. Ingber, *Lab Chip*, 2012, **12**, 2165–2174.
17 S. Kidambi, N. Udpa, S.A. Schroeder, R. Findlan, I. Lee and C. Chan, *Tissue Eng.*, 2007, **13**, 2105–2117.
18 J. W. Song, S. P. Cavnar, A. C. Walker, K. E. Luker, M. Gupta, Y. C. Tung, G. D. Luker and S. Takayama, *PLoS One*, 2009, **4**, e5756.
19 N. J. Douville, Y.C. Tung, R. Li, J. D. Wang, M. E. H. El-Sayed and S. Takayama, *Anal. Chem.*, 2010, **82**, 2505–2511.
20 J. N. Lee, C. Park and G. M. Whitesides, *Anal.Chem.*, 2003, **75**, 6544–6554.
21 M. Shin, K. Matsuda, O. Ishii, H. Terai, M. Kaazempur-Mofrad, J. Borenstein, M. Detmar and J. P.Vacanti, *Biomed. Microdevices*, 2004, **6**, 269–278.
22 J. Shao, L. Wu, Y. Zheng, H. Zhao, Q. Jin and J. Zhao, *Lab Chip*, 2009, **9**, 3118–3125.
23 Y. Liu and M. B. Chan-Park, *Biomaterials*, 2009, **30**, 196–207.
24 K. J. Bayless, H. I. Kwak and S. C. Su, *Nat. Protoc.*, 2009, **4**, 1888–1898.
25 T. A. Ulrich, T. G. Lee, H. K. Shon, D. W. Moon and S. Kumar, *Biomaterials*, 2011, **32**, 5633–5642.
26 H. E. Gruber, G. L. Hoelscher, K. Leslie, J. A. Ingram and E. N. Hanley, *Biomaterials*, 2006, **27**, 371–376.
27 A. Paguirigan and D. J. Beebe, *Lab Chip*, 2006, **6**, 407–413.
28 A. L. Paguirigan and D. J. Beebe, *Nat. Protoc.*, 2007, **2**, 1782–1788.
29 B. M. Gillette, J. A. Jensen, B. X. Tang, G. J. Yang, A. Bazargan-Lari, M. Zhong and S. K. Sia, *Nat. Mater.*, 2008, **7**, 636–640.
30 X. H. Zhang, C. B. Baughman and D. L. Kaplan, *Biomaterials*, 2008, **29**, 2217–2227.
31 S. J. Lee, J. Liu, S. H. Oh, S. Soker, A. Atala and J. J. Yoo, *Biomaterials*, 2008, **29**, 2891–2898.
32 N. Sadr, M. Zhu, T. Osaki, T. Kakegawa, Y. Z. Yang, M. Moretti, J. J. Fukuda and A. Khademhosseini, *Biomaterials*, 2011, **32**, 7479–7490.
33 E. S. Place, D. N. Evans and M. M. Stevens, *Nat. Mater.*, 2009, **8**, 457–470.
34 A. R. Butler and D. L. H. Williams, *Chem. Soc. Rev.*, 1993, **22**, 233–241.
35 C. Nathan, *FASEB J*, 1992, **6**, 3051–3064.

36 B. J. Privett, J. H. Shin and M. H. Schoenfisch, *Chem. Soc. Rev.*, 2010, **39**, 1925–1935.
37 T. Malinski and Z. Taha, *Nature*, 1992, **358**, 676–678.
38 X. Zhang, L. Cardosa, M. Broderick, H. Fein and J. Lin, *Electroanalysis*, 2000, **12**, 1113–1117.
39 Y. Lee, B. K. Oh and M. E. Meyerhoff, *Anal. Chem.*, 2004, **76**, 536–544.
40 N. Diab and W. Schuhmann, *Electrochim. Acta*, 2001, **47**, 265–273.
41 K. Shibuki, *Neurosci. Res.*, 1990, **9**, 69–76.
42 M. Pontie, H. Lecture and F. Bedioui, *Sens. Actuators, B*, 1999, **56**, 1–5.
43 A. Yu, Z. Liang, J. Cho and F. Caruso, *Nano Lett.*, 2003, **3**, 1203–1207.
44 C. Amatore, S. Arbault, Y. Bouret, B. Cauli, M. Guille, A. Rancillac and J. Rossier, *ChemPhysChem*, 2006, **7**, 181–187.
45 Y. Kitamura, T. Uzawa, K. Oka, Y. Komai, H. Ogawa, N. Takizawa, H. Kobayashi and K. Tanishita, *Anal. Chem.*, 2000, **72**, 2957–2962.
46 J. H. Shin, B. J. Privett, J. M. Kita, R. M. Wightman and M. H. Schoenfisch, *Anal. Chem.*, 2008, **80**, 6850–6859.
47 D. H. Kotsis and D. M. Spence, *Anal. Chem.*, 2003, **75**, 145–151.
48 M. Hulvey and R. Martin, *Anal. Bioanal. Chem.*, 2008, **393**, 599–605.
49 W. Cha, Y. C. Tung, M. E. Meyerhoff and S. Takayama, *Anal. Chem.*, 2010, **82**, 3300–3305.
50 L. S. Hu, K. F. Huo, R. S. Chen, X. M. Zhang, J. J. Fu and P. K. Chu, *Chem. Commun.*, 2010, **46**, 6828–6830.
51 F. Y. Du, W. H. Huang, Y. X. Shi, Z. L. Wang and J. K. Cheng, *Biosens. Bioelectron.*, 2008, **24**, 415–421.
52 L. Z. Zhao, L. S. Hu, K. F. Huo, Y. M. Zhang, Z. F. Wu and P. K. Chu, *Biomaterials*, 2010, **31**, 8341–8349.
53 M. V. Klein, J. A. Holy and W. S. Williams, *Phys. Rev. B*, 1978, **17**, 1546–1556.
54 M. Amer, M. W. Barsoum, T. El-Raghy, I. Weiss, S. Leclair and D. Liptak, *J. Appl. Phys.*, 1998, **84**, 5817–5918.
55 A. C. Ferrari and J. Robertson, *Phys. Rev. B: Condens. Matter*, 2000, **61**, 14095–14107.
56 D. D. Thomas, X. Liu, S. P. Kantrow and J. R. Lancaster Jr, *Proc. Natl. Acad. Sci. U. S. A.*, 2001, **98**, 355–360.
57 G. M. Buga, M. E. Gold, J. M. Fukuto and L. J. Ignarro, *Hypertension*, 1991, **17**, 187–193.
58 A. J. Kanai, H. C. Strauss, G. A. Truskey, A. L. Crews, S. Grunfeld and T. Malinski, *Circ. Res.*, 1995, **77**, 284–293.
59 A. M. Andrews, D. Jaron, D. G. Buerk, P. L. Kirby and K. A. Barbee, *Nitric Oxide*, 2010, **23**, 335–342.
60 H. Kojima, Y. Urano, K. Kikuchi, T. Higuchi, Y. Hirata and T. Nagano, *Angew. Chem., Int. Ed.*, 1999, **38**, 3209–3212.
61 L. M. Li, W. Wang, S. H. Zhang, S. J. Chen, S. S. Guo, O. Francais, J. K. Cheng and W. H. Huang, *Anal. Chem.*, 2011, **83**, 9524–9530.

